A NEW SUPERVISED MACHINE-LEARNING-DIVINER BASED APPROACH FOR LUNAR THERMAL EMISSION REMOVAL FOR M^3 HYPERSPECTRAL DATA.

F. Colaiuta[1,2], F. Tosi[2], F. Zambon[2].
[1]Dipartimento di Fisica, Sapienza Università di Roma, Rome, Italy. [2]Istituto Nazionale di Astrofisica – Istituto di Astrofisica e Planetologia Spaziali (INAF-IAPS), Via del Fosso del Cavaliere, Rome, Italy.

Introduction: The Moon Mineralogy Mapper (M^3) enabled the detection of a widespread OH/H_2O absorption signature across the lunar surface. While these features could be partially visible in the raw spectra, accurately constraining the abundance and spatial variability of lunar hydroxyl/water requires the removal of the thermal emission component. The lunar surface temperature can vary significantly over a single lunar day (~100–400 K), depending on multiple factors including latitude, local solar time (LST), solar incidence angle, albedo, regolith thermal emissivity, surface composition, scattering processes, terrain roughness and other local thermophysical properties.

Several approaches have been developed and applied to M^3 data to better quantify surface hydration and to investigate the global- and local-scale processes influencing its formation and preservation. These methods include an M^3 data–driven correction [1], a Diviner-validated, laboratory-derived empirical model [2], and a set of roughness-based thermophysical formulations [3,4]. Although all these techniques support the presence of a pervasive hydration signature on the Moon, the origin of this hydration and its relationship with regolith composition, maturity, and other surface properties remain only partially resolved.

In this framework, we introduce LENNA (*Lunar thermal-Emission Neural Networks Approach*), a thermal emission removal method based on a supervised machine-learning technique, leveraging the extensive archive of Diviner bolometric temperature measurements acquired over the past years.

Methods: The supervised machine-learning framework presented here is based on a feed-forward, fully connected neural-network architecture designed to estimate the lunar surface temperature from several M^3-derived inputs, accounting for potential strong non-linear correlations among parameters. At this stage, the model incorporates the following predictors: latitude, local solar time (LST), solar incidence angle, slope, aspect, reflectance spectrum in the 0.66–2.54µm spectral range (channels 6–74, excluding the region potentially affected by the OH/H_2O absorption feature to better capture compositional, albedo, and thermally driven variations), and the reflectance at channels 74 (~2.54µm) and 49 (~1.55 µm), whose laboratory measurements have shown to be non-linearly correlated [2] and can be used as proxy for thermal emission. The target variable is the bolometric surface temperature.

To train the model, we used bolometric temperature values computed from Diviner observations following [5]. Accordingly, we selected M^3 scenes for which spatially and temporally overlapping Diviner datasets were available, ensuring a wide range of illumination ($0° < i < \sim 85°$), thermal, and morphological conditions to enhance the model's generalization capability. Diviner radiance data were downloaded via the Diviner RDR Query 2.0 [6] and then spatially matched to M^3 using Gaussian interpolation. After reprojection, bolometric temperatures were computed following the formulation proposed by Diviner's team [5].

Radiances were used as the foundational dataset for reprojection because they can be interpolated while preserving energy conservation and physical consistency—an operation that would not be valid if performed directly on bolometric and/or brightness temperatures.

Reflectance spectra thermal correction is performed by modeling the surface emissivity using a radiative transfer model [7], which is more effective in accounting for scatterings and microscopic light behavior with respect to a simple thermal equilibrium formulation based on Kirchhoff's law [2]. The retrieved reflectance uncertainties at channel 81 (~2.86 µm) are always between ± (0.001–0.017), depending on terrain type, illumination geometry and water absorption strength. These values are derived from the LENNA modeled temperature RMSE (*Root Mean Square Error*) of ~4.72 K, obtained for the training set.

Comparison with empirical method and Diviner measurements: We evaluated the performance of our newly developed method across eight ROIs (Regions of Interest), selected to span a wide range of illumination conditions and surface morphologies, including maria/highlands units, pyroclastic deposits, immature highland terrains and craters. The model proves highly effective in removing the thermal component across all tested terrain types, yielding consistently promising results. For example, in the optically immature highland ROI (~45-54°N ~98-103°E) at ~13:00 LST, the method achieves higher accuracy than the laboratory based empirical approach (**Figure 1**), while producing comparable outcomes in other settings. Importantly, the RMSE and standard deviation between the modeled temperatures and the Diviner-derived bolometric temperatures are systematically lower for LENNA. This indicates that, although the average retrieved spectra are similar to those obtained with the Li and Milliken empirical method [2], LENNA seems to provide a more accurate and stable temperature estimation at the pixel scale.

To better assess the accuracy of the method, we apply LENNA on a global scale using a small number of M^3 data selected to sample all latitudes and terrain types. The results show that LENNA is in very good agreement with the independent Diviner latitudinal trend [8] over the full range of LSTs sampled during the M^3 acquisition period (e.g., **Figure 2**).

We further evaluate its ability to capture anisothermal effects by comparing our results with the Diviner channel 3 brightness temperature (**Figure 3**). LENNA appears to partially resolve anisothermal effects even at high incidence angles, potentially overcoming the precision and accuracy of the Li and Milliken method [2].

Acknowledgments: The authors acknowledge support from the Space It Up project, funded by the Italian Space Agency and the Italian Ministry of University and Research. Contract n. 2024-5-E.0 – CUP n. I53D24000060005.

References: [1] Clark, R.N. et al. (2011) *Journal of Geophysical Research, Planets, 116(E6).* [2] Li, S. & Milliken, R.E. (2016) *Journal of Geophysical Research, Planets, 121(10).* [3] Wohlfarth, K. et al. (2023) *Astronomy & Astrophysics, 674(A69).* [4] Wöhler, C. et al. (2017) *Science advances, 3(9).* [5] Paige, D.A. et al. (2010) *Science, 330(6003)*. [6] PDS Geosciences Node's Granular Data System Diviner RDR Query Tool, Version 2.0. https://oderest.rsl.wustl.edu/GDSWeb/GDSDLRERDR.html. [7] Hapke, B. (2005) *Theory of Reflectance and Emittance Spectroscopy.* [8] Williams, J.–P. et al. (2017) *Icarus, 283(300-325).*

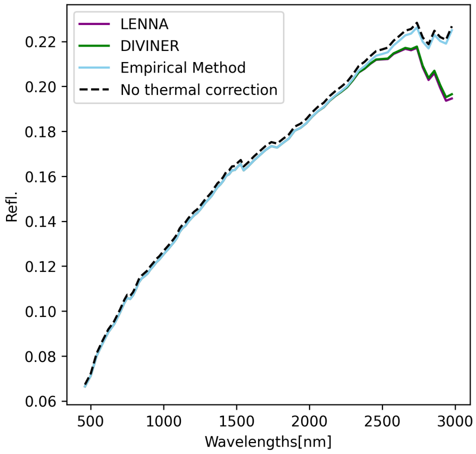

Figure 1: Average reflectance spectra for highly immature highland (~45-54°N ~98-103°E) at ~13:00 LST. The average spectrum thermally corrected with LENNA (purple) coincides with the one retrieved via Diviner's temperatures (green). The Li and Milliken empirical method is reported in lightblue.

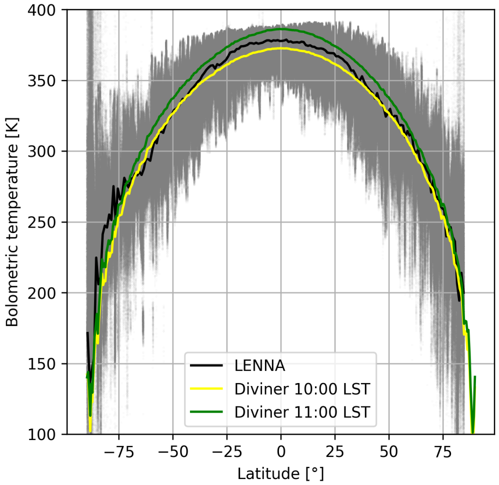

Figure 2: Latitudinal trend for LENNA modeled temperatures and Diviner results [7] between 10:00 LST and 11:00 LST.

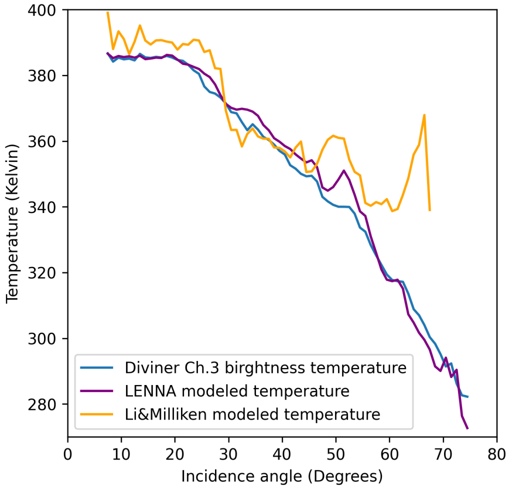

Figure 3. Bolometric temperatures derived using LENNA (purple), Li and Milliken empirical method (orange) [2] and the channel 3 Diviner brightness temperatures along with the incidence angles for a subset of M^3 observations. LENNA modeled temperatures appear to be more effective in representing potential anisothermal effects at high incidence angles ($i > 55°$).